SPIN CODE BENCHMARKING AT RHIC*

F. Méot, M. Bai, V. Ptitsyn, V. Ranjbar
Collider-Accelerator Department, BNL, Upton, NY 11973, USA.

Abstract

Stepwise ray-tracing methods are being developed at C-AD, BNL, in view of benchmarking of existing spin codes and of spin dynamics simulations at RHIC. A status of that work is reported here.

INTRODUCTION

Stepwise ray-tracing appears to perform well for particle and spin tracking in rings, because it combines high accuracy regarding the modeling of magnetic and electric fields in lattice optical elements, with high accuracy of the integration method.

The ray-tracing code Zgoubi [1] is being used and developed in view of benchmarking of existing spin codes [2] and of spin dynamics simulations at RHIC. Earlier publications have shown its efficiency in performing that task [3].

This paper reports on the present status of these benchmarking exercises and simulations.

Table 1: RHIC Parameters, Nominal Tunes

	MAD	Zgoubi[(1)]
Orbit length (m)	3833.8452	3833.8459
Qx, Qy	28.6950, 29.6850	28.6850, 29.6750
Q'x, Q'y	2, 2	1.76, 2.62
α, $\sqrt{1/\alpha}$	0.001788, 23.647	0.001796, 23.597
Periodic functions at "Clock 6":		
β_x, β_y (m)	0.70, 0.72	0.98, 1.02
α_x, α_y	-0.04, 0.02	-0.03, 0.02
Snake 1, snake 2 data :		
Spin rotation (deg.)	180, 180	
Axis angles (deg.)	90, 0 [(2)]	

[1] MAD's 'SBEND' is simulated using 'BEND' in Zgoubi, other lenses are simulated using 'MULTIPOL'[1]. Differences between the two sets of data still need investigation.
[2] Note: $+/-45$ degrees instead, in RHIC operation.

MODELING OF RHIC

The input data to Zgoubi is obtained by prior MAD run, then a translator takes care of the rest. In this paper we consider the blue ring, data in Tab. 4. The two snakes are simulated as a point transform on spin, no effect on beam (unlike AGS case [3]).

In order to complete this overview of the working conditions, and as a benchmarking exercise as well, strongest intrinsic resonances ($|J_n|^2/\epsilon_x/\pi > 10^5$) are displayed in Fig. 1, together with theoretical thin-lens model data:

$$\frac{J_n^{\pm}}{\sqrt{\epsilon_z/\pi}} = \frac{1+\gamma G}{4\pi}\Sigma_{Quads}\left\{\begin{array}{c}\cos(\gamma G\alpha_i \pm \psi_i)\\ \sin(\gamma G\alpha_i \pm \psi_i)\end{array}\right\}(KL)_i\sqrt{\beta_{z,i}} \quad (1)$$

* Work supported by Brookhaven Science Associates, LLC under Contract No. DE-AC02-98CH10886 with the U.S. Department of Energy.

and their difference, for comparison.

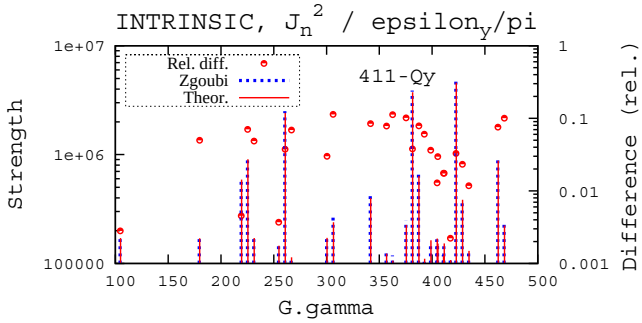

Figure 1: Strength of intrinsic resonances, from ray-tracing, and theoretical values (Eq.1).

DEFECT AND CHROMATIC ORBIT

Spin tracking regarding defect or chromatic closed orbit induced δQ_s is addressed here, following developments in Ref. [4, 5]. The goal is to provide data for comparison with UAL-Spink [6].

The $G\gamma = 411 - Q_y$ intrinsic depolarizing resonance energy region is considered (Fig. 1), near $Q_{y,snk} = \frac{2m+1}{2n} = \frac{7}{10}$ odd snake resonance.

Working Conditions

Intrinsic resonance environment is as shown in Fig. 1. Working conditions accounted for in Zgoubi are given in Tab. 4, but for the tunes liable to further adjustment depending on the "numerical experiment".

The energy is ramped across $411 - Q_y$, typical behavior of the vertical component of the polarization is as displayed

Table 2: Orbit Data, Geometric and Chromatic, $G\gamma = 411 - Q_y$ Region

Q_x	28.6977
Q_y	29.6726
Q_s (kick off, snakes off)	0.26695
Q_s (kick on, snakes off)	0.26693
Geometrical orbit data:	
x'_{co}/x'_K at snake 1	-1.248
x'_{co}/x'_K at snake 2	$+0.983$
Expected $\left\vert\frac{Q_s-0.5)}{\Delta x'_{co,snake}}\right\vert_{geom.} = \frac{G\gamma+1}{\pi}$	120.72
Chromatic orbit data:	
D'_x at snake 1 (mrad)	$+9.5$
D'_x at snake 2 (mrad)	-46
Expected $\left\vert\frac{Q_s-0.5)}{\Delta D'_{x,snake}\delta p/p}\right\vert = \frac{G\gamma+1}{\pi}$	120.4

in Fig. 5. Spin tune Q_s is obtained from Fourier analysis of a few 100s turn in the vicinity of the resonance. Horizontal closed orbit (sample in Fig. 2) is introduced using an horizontal corrector located 1137.3313m from "clock6", yielding a difference in angles $\Delta x'_{co,snake}/x'_K$ at snakes. The horizontal dispersion function is displayed in Fig. 3.

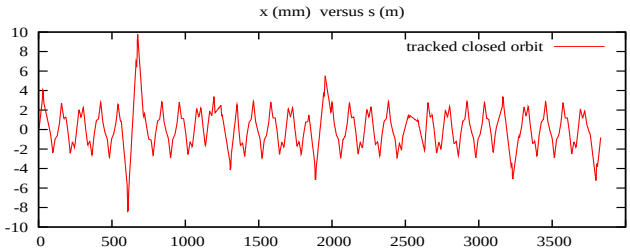

Figure 2: Typical closed orbit, for $x'_K = -10^{-4}$ rad.

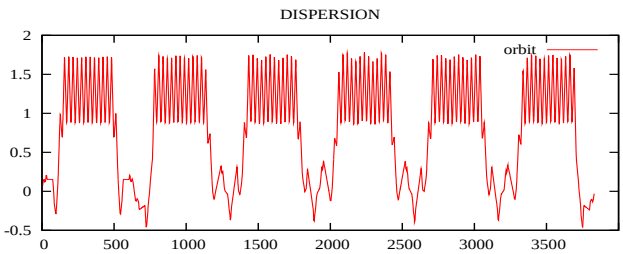

Figure 3: Dispersion.

Defect Closed Orbit

Four different values of the horizontal kick x'_K are considered. The initial spin vector (at clock6) is taken at degrees from $\vec{y}$ to allow accurate computation of Q_s from Fourier analysis, whereas starting $G\gamma$ is taken far enough from the resonance, close to a node of $S_y(G\gamma)$, see Fig. 5. Table 3 clearly shows that the spin tune is shifted from 0.5 by the expected value, $\delta Q_s = \frac{G\gamma+1}{\pi}\Delta x'_{co,snake}$ [4, Eq. 7].

The second part of Table 3 shows that sextupoles do not have sensible effect on this result.

Table 3: Closed Orbit Defect Spin Tune Effects

x'_K (rad)	0	-10^{-5}	-10^{-4}	-10^{-3}
$\Delta x'_{co,snake}$ (mrad)	0	0.02235	0.2231	2.1563
Qs	0.5	0.5027	0.5269	0.2396
$\left\lvert\frac{Q_s-0.5}{\Delta x'_{co,snake}}\right\rvert$		120.2	120.5	120.7
All sextupoles off:				
$\Delta x'_{co,snake}$ (mrad)			0.2235	
Qs			0.4730400	
$\left\lvert\frac{Q_s-0.5}{\Delta x'_{co,snake}}\right\rvert$			120.6	

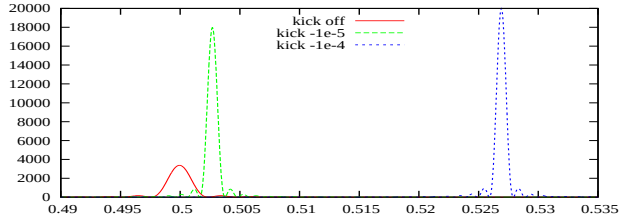

Figure 4: Spin spectrum ($\frac{\sin x}{x}$ effect stems from sampling).

Chromatic Closed Orbit

Three different $\delta p/p$ values are considered. Table 4 shows that the spin tune is shifted from 0.5 by the expected value [5, Eq. 5] $\delta Q_s = \frac{G\gamma+1}{\pi}\Delta D'_{x,snk}\frac{\delta p}{p}$.

Table 4: Chromatic Closed Orbit Spin Tune Effects

$\delta p/p$	10^{-4}	10^{-3}	10^{-2}
x'_{ch} at snake 1 (mrad)	+0.00095	+0.00916	+0.1195
x'_{ch} at snake 2 (mrad)	−0.00457	−0.045164	−0.3301
$\Delta D'_{x,snake}$ (rad)	0.0552	0.0543	0.04496
Qs	0.4993	0.4934	0.4452
$\left\lvert\frac{Q_s-0.5}{\Delta D'_{x,snake}\delta p/p}\right\rvert$	121.4	121.0	122.0

Resonance Crossing Near Snake Resonance

Crossing of the snake resonance object of the studies above is part of the benchmarking. The energy range explored is at $G\gamma = 411 - Q_y$ resonance, close to $Q_{y,snk} = \frac{2m+1}{2n} = 7/10$ odd snake resonance. $Q_y = 29.6750$ here, yielding $G\gamma|_{resonant} = 381.325$.

Single particle (Fig. 5) The tracking locates the extremum of S_y at $(411 - Q_y) - G\gamma \approx 0$ (Fig. 5-top), as expected. Separation between the side nodes is as expected ≈ 2 units of $G\gamma$ with 2 the number of snakes [7, p.102].

The envelope $< \bar{S}_y >= 1 - 8(1-b^2)b^2$, $b = \frac{\pi|\epsilon|}{2}\frac{\sin \pi\lambda/2}{\pi\lambda/2}$ with $\lambda = \sqrt{\delta^2 + |\epsilon|^2}$, δ =distance to the resonance, ϵ =resonance strength, is from [7, Eq. 5.37] with amplitude normalized to Zgoubi data.

Synchrotron motion with large $\widehat{dp/p} = 8\times10^{-4}$ (Fig. 5-bottom) does not substantially change $< \bar{S}_y >$ pattern neither the recovering of $<S_y>$, due to the tune remaining far from 7/10.

32 particle sample (Fig. 6) 32 particles are taken with initial conditions:

- ϵ_x =constant 3π mm-mrad, normalized;
- dp/p=0;
- vertical coordinates at $2\pi/8$ phase interval on four different invariants, simulating a Gaussian distribution [9]. Fig. 6 shows the transmission of the average $<S_y>$ over $E = 230 \rightarrow 250$ GeV.

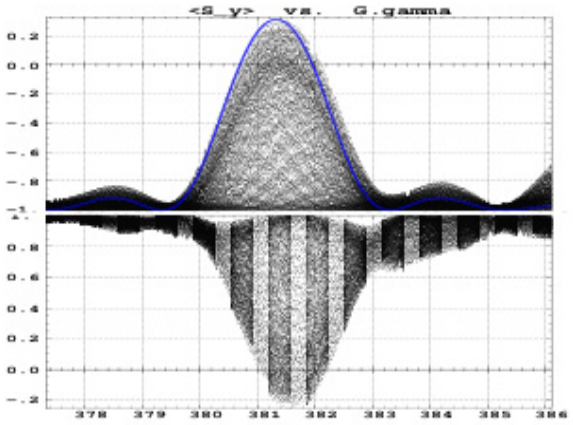

Figure 5: Crossing $411 - Q_y$, snakes on, single particle, $\epsilon_y/\pi = 2.6$ mm-mrad normalized. Top: on-momentum, observed at the snake ("snake 1"); bottom: including synchrotron motion, $\widehat{dp/p} = 8 \times 10^{-4}$, observation point is clock 6, away from the snakes hence loss of symmetry [8].

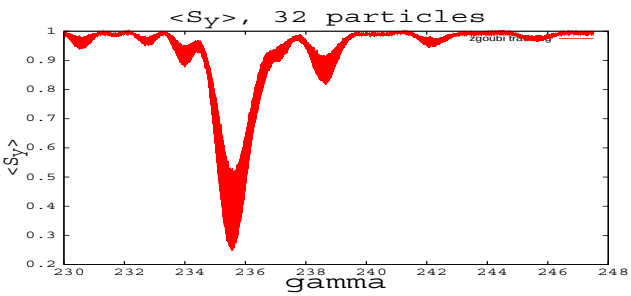

Figure 6: Ramping from $E = 230 \rightarrow 250$ GeV, 32 particles, average $< S_y >$.

Nearing 7/10 Odd Snake Resonance

The snake resonance location in presence of spin tune shift δQ_s satisfies [10] $Q_{y,snk} = \frac{2m+1}{2n} \pm \frac{\delta Q_s}{n}$.

$Q_{y,snk} = 7/10 \pm \frac{\delta Q_s}{n}$ may be attained via, on the one hand, effect of chromaticity $Q_y = Q_{y0} + \xi_y \frac{\delta p}{p}$, on the other hand $\delta p/p$ induced spin tune shift ([5, Eq. 5]) liable to reach $\delta Q_s \approx 0.003$ given $\Delta D'_{x,snake} \approx 55$ mrad (Tab. 2), while taking an upper value $\delta p/p \approx 5 \times 10^{-4}$.

However, in the present simulation conditions the longitudinal acceptance sets a limit of $\delta p/p \approx 2.4 \times 10^{-4}$. Therefore, the chromaticity is increased to $\xi_y = 22$ instead - far beyond the nominal value of 2, Tab. 4. The fractional vertical betatron tune is then varied from 0.680 to 0.695, so to explore the immediate vicinity of $Q_{y,snk} = 7/10$.

Fig. 7, with initial particle transverse invariants as in Fig. 5, shows how $< S_y >$ is affected by the proximity of the resonance. The bottom plot shows that the effect can be correlated to Q_y overlapping $Q_{y,snk}$.

This is an on-going work, investigations and theoretical understanding efforts will be carried on.

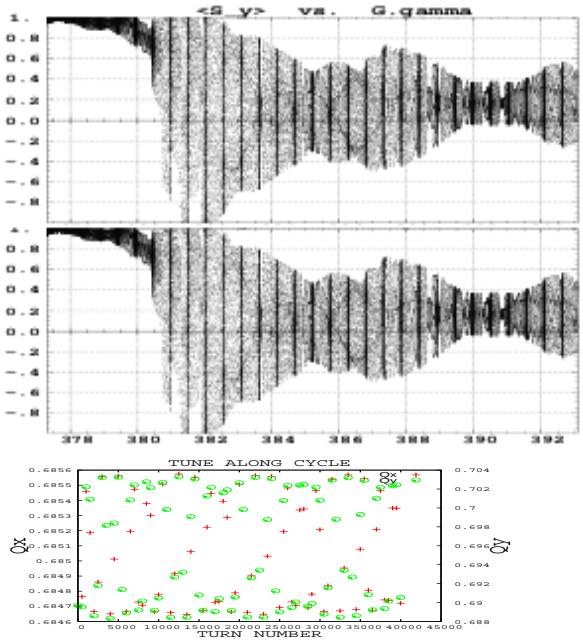

Figure 7: Depolarization upon crossing $411 - Q_y$, single particle. Top: initial $dp/p = 2.4 \times 10^{-4}$, middle: initial $dp/p = -2.4 \times 10^{-4}$. Bottom: tunes along the ramp.

REFERENCES

[1] The ray-tracing code Zgoubi, F. Méot, NIM-A 427 (1999) 353-356; http://sourceforge.net/projects/zgoubi/

[2] Spin tracking with GPUs to 250 GeV in RHIC lattice, V. Ranjbar et al., WEP141, these proceedings.

[3] Development of a stepwise ray-tracing based on-line model at AGS, F. Méot et al., WEP141, these proceedings.

[4] Impact on Spin Tune From Horizontal Orbital Angle Between Snakes and Orbital Angle Between Spin Rotators, M. Bai, V. Ptitsyn, T. Roser, C-A/AP/334 Note (10/08).

[5] Spin Tune Dependence on Closed Orbit in RHIC, V. Ptitsyn, M. Bai, T. Roser, THPE054, IPAC 2010, Kyoto.

[6] Spin tracking in RHIC - Code SPINK, A.U. Luccio, Proc. Conf. "*Trends in Collider Physics*", Trieste, Italy (1995).

[7] Spin dynamics and snakes in synchrotrons, S. Y. Lee, World Scientific (1997).

[8] Polarized beams in accelerators and storage rings with Siberian Snakes, V. Ptitsyn, Ph.D. thesis, Novosibirsk, Russia (1997).

[9] Overcoming intrinsic spin resonances using an RF dipole, M. Bai, PhD Thesis, UMI (1999).

[10] Orbit effects on polarization in RHIC, V. Ptitsyn, RHIC MAC, Nov. 2010.